单晶TiO2纳米颗粒实现高效稳定钙钛矿模块

作者：writer 来源：爱科学

本文原地址：https://www.iikx.com/news/progress/18091.html

本文仅供学习交流之用，版权归原作者所有，请勿用于商业用途！

单晶TiO2纳米颗粒实现高效稳定钙钛矿模块。
近日，华北电力大学戴松元团队/西安交通大学杨冠军团队/洛桑联邦理工大学M. K. Nazeeruddin团队等利用一步溶剂热法合成出菱形单晶TiO2纳米颗粒，并将其用于钙钛矿太阳电池中的介孔电荷传输层，有效降低了器件光电损耗，并提高了小面积电池的效率（24.05%）和填充因子（84.7%）。

2022年4月21日，该研究以Single-crystalline TiO2 nanoparticles for stable and efficient perovskite modules为题，发表在Nature Nanotechnology上。论文第一作者为丁勇、丁斌，通讯作者为杨冠军、戴松元、Paul. J. Dyson、Mohammad Khaja Nazeeruddin。

有机-无机杂化钙钛矿太阳电池经过10余年的快速发展，高达25.7%的认证效率可媲美于商业化晶硅太阳电池。但组件效率与实验室小尺寸电池依然存在较大差距，主要来源于电荷传输层电阻高、电荷传输层/钙钛矿界面以及大面积钙钛矿薄膜内部缺陷多所导致的光电损耗。因此，如何制备高品质电荷传输层和钙钛矿薄膜、降低层内和界面损耗，是当前面临的重大挑战。

华北电力大学戴松元团队/西安交通大学杨冠军团队/洛桑联邦理工大学M. K. Nazeeruddin团队等利用一步溶剂热法合成出菱形单晶TiO2纳米颗粒，并将其用于钙钛矿太阳电池中的介孔电荷传输层，借助TiO2纳米菱的高结晶度、低密度缺陷态、高电导率、高晶格匹配度及其与钙钛矿的高亲和力，有效降低了器件光电损耗，进而提高了小面积电池的效率（24.05%）和填充因子（84.7%）。

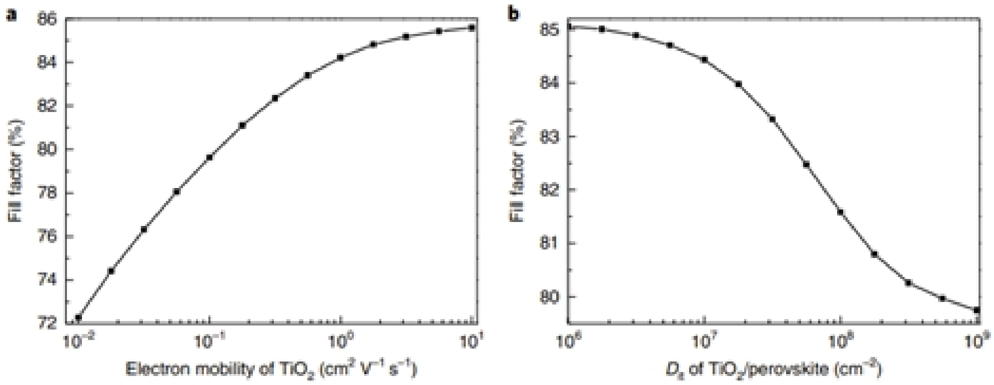

Fig. 1 | Effects of electron mobility of TiO_2-based ETL and interfacial defect density of TiO_2/perovskite interface on the FF loss. a, Electron mobility effect. **b**, Interfacial defect density effect.

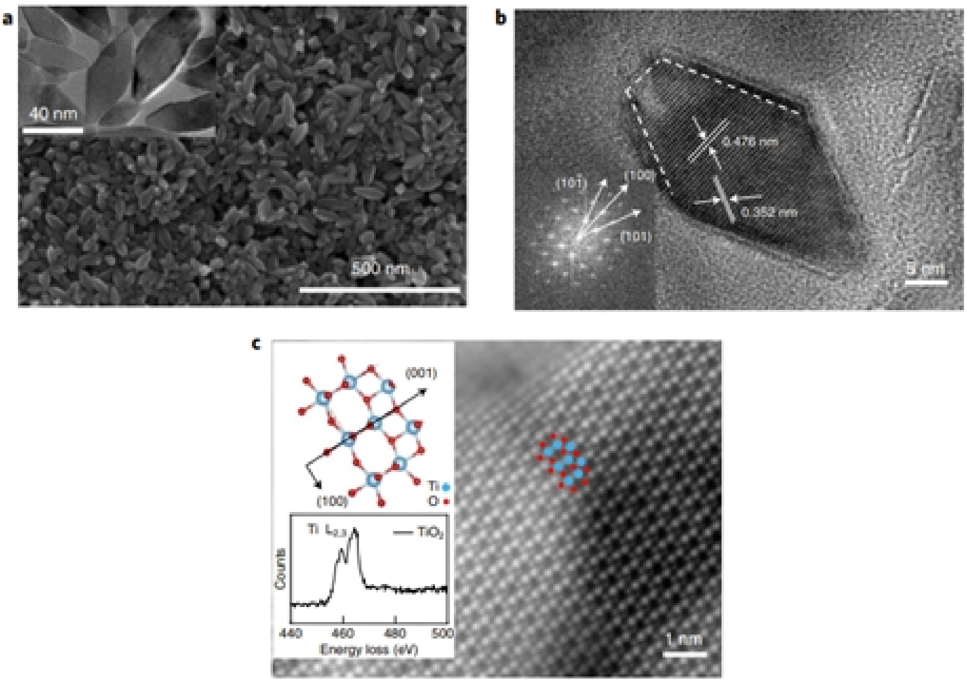

Fig. 2 | Morphology and characterization of single-crystalline TiO_2 nanoparticles. a, SEM image. The inset shows a TEM image of the SC. **b**, High-resolution TEM image. The inset displays a fast Fourier transform image, suggesting it is a single crystal. The dashed line shows the edge of rhombohedral nanoparticles. **c**, Spherical aberration electron microscopy image. The top inset illustrates the crystal structure along the [010] axis), and the bottom inset shows an electron energy-loss spectrum of the SC, demonstrating the highly crystalline nature of the SC.

鉴于目前实验室广泛采用旋涂与反溶剂技术制备钙钛矿吸光层，但在除溶剂过程中，旋出的反溶剂会造成大面积钙钛矿薄膜出现针孔和/或裂纹缺陷，直接抑制电荷提取并导致陷阱态复合，限制了高品质钙钛矿薄膜的大面积制备。作者团队利用自主发展的真空抽气法制备出高品质钙钛矿薄膜，该方法更适合批量制备大面积钙钛矿薄膜。据此，制备出有效面积24 cm2的大面积组件，认证效率达到22.72%，显著缩小了大组件与小电池的效率差距。

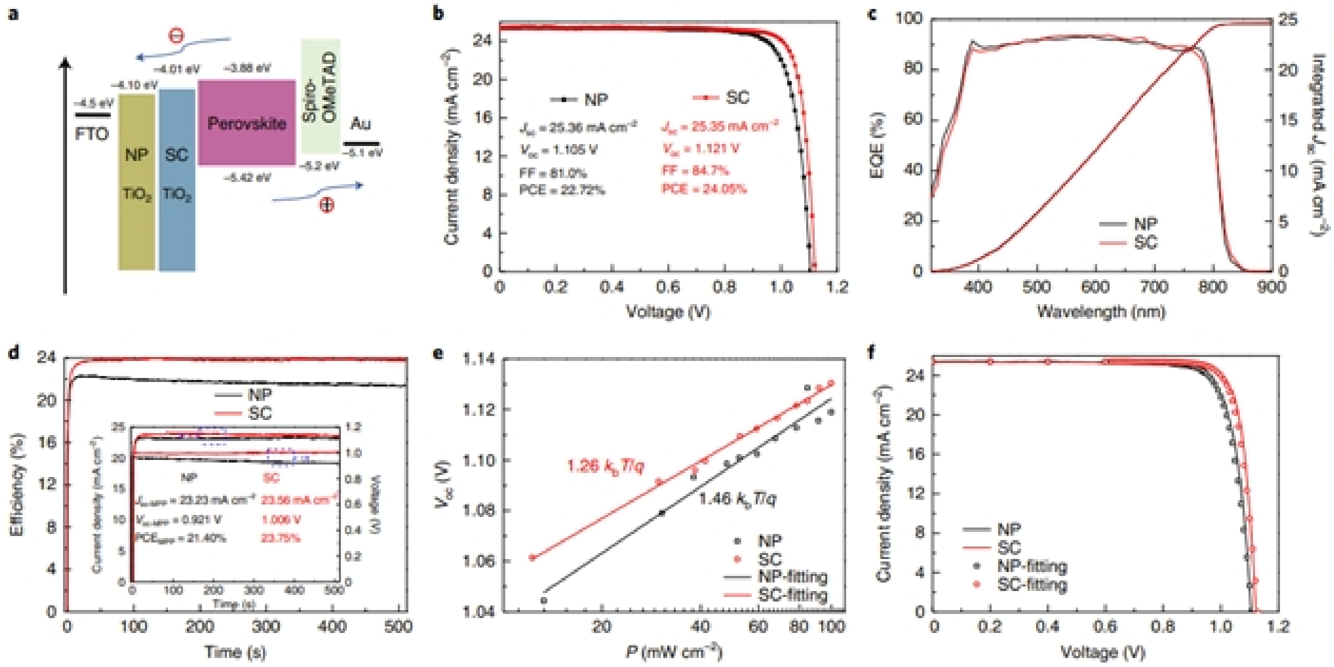

Fig. 3 | Comparison of NP- and SC-based device photovoltaic performance and characterization. a, Energy band level of the devices. **b**, *J–V* curves of the best performing devices for each condition measured from reverse scan under simulated air mass 1.5 (AM1.5) sunlight. The devices were covered with an antireflection film and a metal mask with an area of 0.09 cm^2. **c**, EQE spectra and integrated photocurrent curve of the devices. The integrated J_{sc} values over the entire EQE spectra were 24.55 and 24.58 mA cm^{-2} for the NP- and SC-based devices, respectively. **d**, Stabilized power output measured for 500 s at the maximum power point (MPP). The inset shows the steady-state current and voltage measurement. **e**, V_{oc} dependence of light intensity with ideality factors n_{id}. **f**, Simulation of electron mobility and interfacial defect density (D_{it}) effect on the performance. The solid lines represent experiment data, and the open squares denote the simulation.

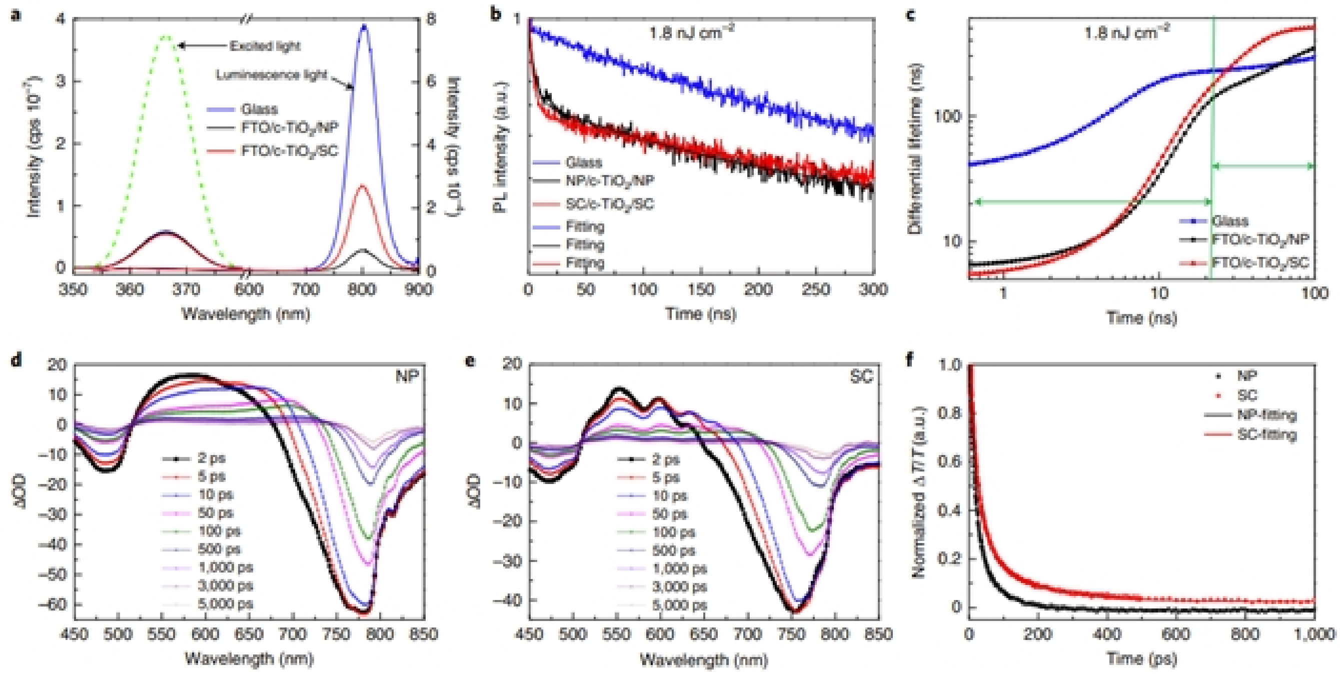

Fig. 4 | Interfacial charge transfer dynamics of perovskite films based on the NP and SC substrates. a, PLQY of perovskite films deposited on the glass, FTO/c-TiO_2/NP and FTO/c-TiO_2/SC substrates. **b**, Time-resolved photoluminescence (PL) measurements of perovskite films deposited on the glass, FTO/c-TiO_2/NP and FTO/c-TiO_2/SC substrates. **c**, Corresponding differential lifetime of perovskite films deposited on the glass, FTO/c-TiO_2/NP and FTO/c-TiO_2/SC substrates. **d**,**e**, Transient absorption spectra at different delay times of FTO/c-TiO_2/NP/perovskite (**d**) and FTO/c-TiO_2/SC/perovskite (**e**) films. ΔOD, change in absorbance. **f**, Normalized transient absorption kinetic profiles probed at 750 nm of FTO/c-TiO_2/NP/perovskite and FTO/c-TiO_2/SC/perovskite films.

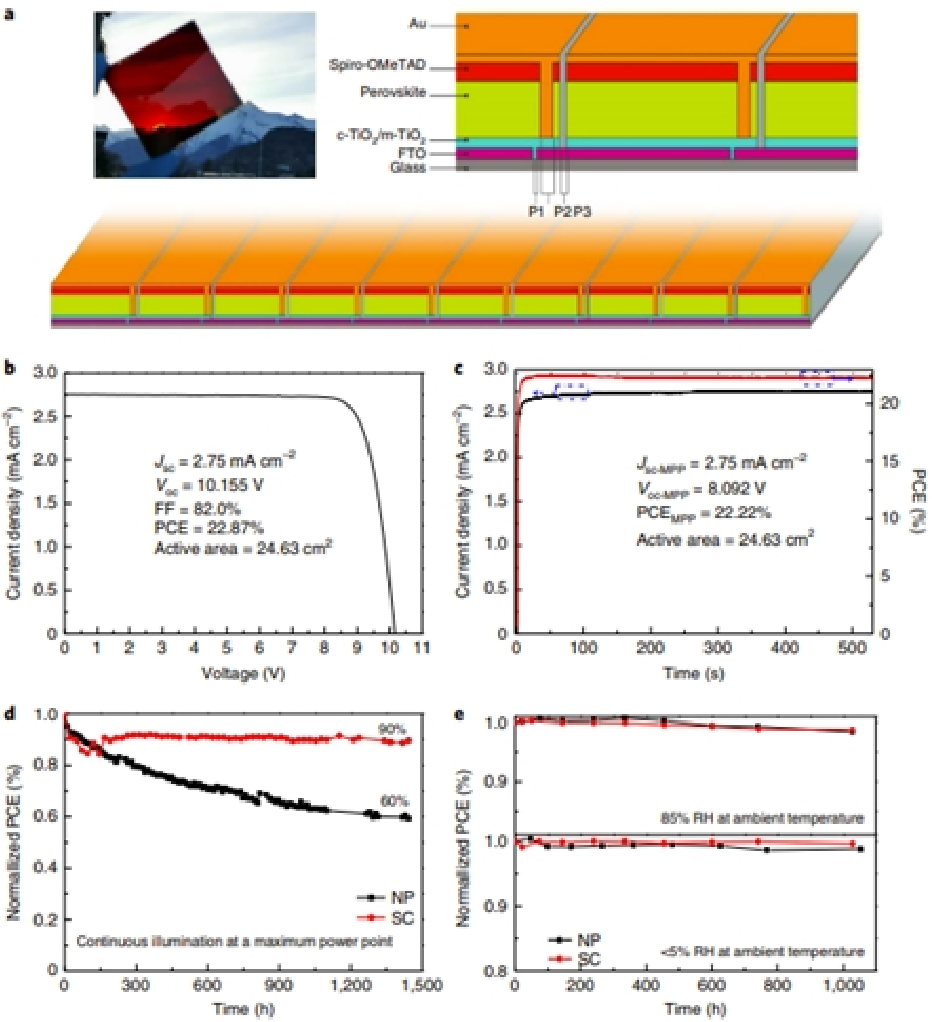

Fig. 5 | Module architecture and performance, and small-sized device's stability. a, Schematic of module structure with nine subcells connected in series. The inset shows a photograph of unencapsulated FTO/c-TiO_2/NP/perovskite/spiro-OMeTAD film. P1, P2 and P3 refer to the laser scribing process in the module fabrication. **b**, Champion *J*–*V* curve of a module in reverse scanning mode. **c**, The stabilized photocurrent output and PCE of a module under maximum power point. **d**, Operation stability of small devices without encapsulation measured at a maximum power point under a continuous AM1.5G light-emitting diode light illumination in a N_2 box with a relative humidity (RH) below 5%. **e**, Humidity stability of small-sized devices encapsulated under a relative humidity of 85% and a relative humidity of <5% in a drying box.

上述研究显示，设计电子传输层菱形单晶结构和发展钙钛矿层抽气制备方法，为提高大面积组件效率、推动钙钛矿光伏产业化发展提供了新的技术路线。（来源：科学网）

相关论文信息：https://doi.org/10.1038/s41565-022-01108-1

作者：戴松元等 来源：《自然-纳米技术》

更多 科学进展 请访问 https://www.iikx.com/news/progress/

本文版权归原作者所有，请勿用于商业用途，爱科学iikx.com转发